

On the role of CO formation during the aerobic oxidation of alcohols on Pd/Al₂O₃: an in situ attenuated total reflection infrared study

Csilla Keresszegi, Davide Ferri, Tamas Mallat, Alfons Baiker*

Department of Chemistry and Applied Biosciences, Swiss Federal Institute of Technology, ETH Hönggerberg, CH-8093 Zurich, Switzerland

Received 20 January 2005; revised 13 May 2005; accepted 21 May 2005

Available online 14 July 2005

Abstract

Dehydrogenation and oxidative dehydrogenation of six different primary and secondary, aliphatic and aromatic alcohols to the corresponding carbonyl compounds were studied in cyclohexane, in the presence and absence of air. The reaction network was examined by attenuated total reflection infrared (ATR-IR) spectroscopy of the catalytic solid–liquid interface and by GC analysis of the effluent in a continuous-flow reactor. The 5 wt% Pd/Al₂O₃ catalyst was located in an ATR-IR cell that served as a tiny reactor. The studies revealed that all aldehydes formed from primary alcohols (1-octanol, benzyl and cinnamyl alcohol) decarbonylated on Pd, whereas the ketones (2-octanone, cyclohexanone, and acetophenone) were stable. The decarbonylation reactions indicated by IR and the hydrogenation and hydrogenolysis-type side reactions detected by GC even in the presence of molecular oxygen corroborated the presence of surface Pd⁰ sites and the classic dehydrogenation mechanism of alcohol oxidation. Moreover, the facile removal of CO and the phenyl radical formed from decarbonylation of benzaldehyde during benzyl alcohol oxidation unambiguously proved the simultaneous presence of adsorbed oxygen and hydrogen on the Pd surface. The relatively high rate of benzyl alcohol oxidation is attributed to the faster removal of strongly adsorbed by-products from the metal surface and partly to the highest polarity of this alcohol among all of the reactants investigated. Benzyl alcohol increases the solubility of water in the apolar solvent and thus minimizes the negative effect of water coproduct that accumulates on the catalyst surface.

© 2005 Elsevier Inc. All rights reserved.

Keywords: Pd/alumina; Dehydrogenation; Aerobic oxidation; Decarbonylation; In situ ATR-IR spectroscopy; Benzyl alcohol; 1-Phenylethanol; 2-Octanol; Cyclohexanol; 1-Octanol; Cinnamyl alcohol

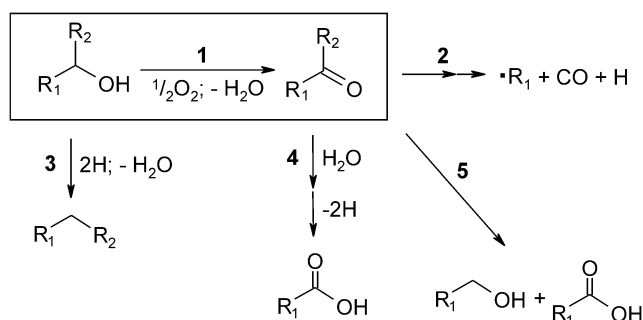
1. Introduction

Much attention has been paid recently to in situ spectroscopic methods in the study of the catalytic solid–gas and (to a smaller extent) the solid–liquid interface [1,2]. Among other techniques, attenuated total reflection infrared (ATR-IR) spectroscopy [3] is a powerful tool for gaining insight into heterogeneous catalytic processes at a molecular level [4–10]. Here we applied this technique to investigate the catalytic processes occurring at the Pd/Al₂O₃–liquid interface during oxidation of alcohols with molecular oxygen (Scheme 1, reaction 1). In contrast to the extensive research on alcohol–Pd and carbonyl compound–Pd interactions on

Pd single crystal surfaces under UHV conditions [11–13], ATR-IR makes it possible to probe these interactions with a commercial Pd/Al₂O₃ powder catalyst and an organic solvent as a reaction medium.

Aerobic oxidation of alcohols over Pt-group metal catalysts in water or organic solvents is an environmentally attractive and industrially relevant process [14–16]. According to the mostly accepted dehydrogenation mechanism of the reaction, the role of oxygen is to oxidize the coproduct hydrogen [17–19]. As a consequence of this mechanism, the active metal is in a metallic state, partially covered by hydrogen [20–23]. On the other hand, there are several reports suggesting that surface oxygen is directly involved in the interaction with the adsorbed alcohol or its partially dehydrogenated intermediate [24]. It has also been proposed that Pd oxide would be the real active species, and its reduc-

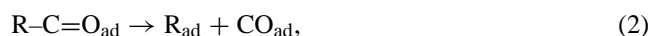
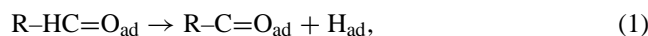
* Corresponding author. Fax: +41-1-632-11-63.
E-mail address: baiker@chem.ethz.ch (A. Baiker).



Scheme 1. Generalized reaction scheme for the transformation of alcohols on Pd/Al₂O₃. 1, oxidative dehydrogenation; 2, decarbonylation (if R₂ = H); 3, C–O bond hydrogenolysis; 4, hydration–dehydrogenation (if R₂ = H); and 5, Cannizzaro reaction (if R₂ = H). All species are considered as adsorbed either on the metal surface or on the support, and the reactions are catalyzed by Pd except for reaction 5 that is catalyzed by Al₂O₃.

tion to Pd⁰ by the alcohol reactant would result in catalyst deactivation [25]. Note the contradiction of this concept to the thoroughly investigated phenomenon referred to as catalyst “overoxidation” [26,27]. As has been shown repeatedly, too high an oxygen concentration can lead to successive oxidation of the metal surface and a drop in activity. This difficulty can be avoided simply by working in the mass-transport-limited regime and thus keeping the metal surface in a reduced state [28,29].

The mechanistic studies may be complicated by an important side reaction, the decomposition of the carbonyl compound product [Eqs. (1)–(4)]. The strongly adsorbed CO can be removed by oxidation with adsorbed oxygen, whereas removal of the hydrocarbon residue necessitates reducing conditions [30,31]:



The decarbonylation reaction over Pt-group metals has been studied extensively by temperature-programmed desorption [32], high-resolution electron energy loss spectroscopy [13,33], and spectroelectrochemical methods [34,35]. Despite the special conditions applied (single crystal metal surfaces under UHV conditions and extended polycrystalline metal surfaces in strongly acidic medium, respectively), the observations also seem to be relevant for the aerobic oxidation of alcohols in water or organic solvents [9,36]. We have shown by ATR-IR spectroscopy under working conditions that cinnamaldehyde and benzaldehyde decarbonylate on Pd/Al₂O₃ [10,37].

Here we extended the range of reactants involving primary and secondary aliphatic (1-octanol, 2-octanol), cycloaliphatic (cyclohexanol), aromatic (benzyl alcohol, 1-phenylethanol), and allylic (cinnamyl alcohol) alcohols. The aim of the work is to confirm the dehydrogenation

mechanism of alcohol oxidation and to unveil the role of alcohol structure in the product degradation. We followed the reactions with a combination of in situ ATR-IR spectroscopy of the catalytic surface and GC analysis of the effluent of the reactor cell.

2. Experimental

2.1. Materials

1-Phenylethanol (Aldrich and Acros, 98%), 2-octanol (Fluka, ≥ 99.5%), cyclohexanol (Merck, > 99%), 1-octanol (Fluka, ≥ 99.5%), benzyl alcohol (Aldrich, > 99%), acetophenone (Fluka, ≥ 99%), 1-octanal (Fluka, ≥ 98%), high-purity water (Merck), and cyclohexane solvent (Aldrich, > 99%) were used as received. Cinnamyl alcohol (Acros, 98%) was purified by recrystallization from petroleum ether. Synthetic air, hydrogen, and Ar were of 99.999 vol% grade (PANGAS), whereas a 0.5 vol% CO in Ar (PANGAS) was used for the study of CO adsorption. The 5 wt% Pd/Al₂O₃ (Johnson Matthey 324) possessed a monomodal particle size distribution in the range of 1–6 nm. The mean Pd particle size (3.4 nm) was determined by TEM; the corresponding Pd dispersion was 0.34 [38].

2.2. ATR-IR spectroscopy: dehydrogenation in a continuous reactor

The 2-mm-thick trapezoidal ZnSe internal reflection element (IRE, 45°, 50 × 20 × 2 mm, Komlas) was coated with Pd/Al₂O₃ by dropping on its larger side an aqueous slurry of the catalyst, as reported elsewhere [10]. After evaporation of the solvent under vacuum, the excess material was removed to match the geometric area of approximately 40 × 7 mm². The ATR cell is designed in such a way that the solution can only flow over that part of the IRE that is covered by the catalyst. Because of the porosity of the catalyst layer, a minor contribution to the ATR-IR spectra from the exposure of the reaction mixture to ZnSe cannot be ruled out. The amount of catalyst was 10 ± 1 mg, which formed a layer of ca. 85 μm, as determined by scanning electron microscopy (SEM, Fig. 1). An approximate penetration depth (*d_p*) of 0.9 μm was calculated with the following formula [3]:

$$d_p = \frac{\lambda/n_{\text{IRE}}}{2\pi\sqrt{\sin^2\theta - (n_1/n_{\text{IRE}})^2}}, \quad (5)$$

assuming that 1/λ = 1700 cm⁻¹ (ν(C=O) of ketones and aldehydes), *n*_{IRE} = 2.4, *n*₁ = 1.3 (wet catalyst layer), and θ = 45°. This indicates that only about 1% at the bottom of the catalyst layer is probed by the evanescent wave generated by the IR beam at the IRE–catalyst interface. This geometry represents a certain drawback when we consider the possible diffusion limitation through the pores visible in the inset of Fig. 1 [10]. Note that a relatively thick layer is

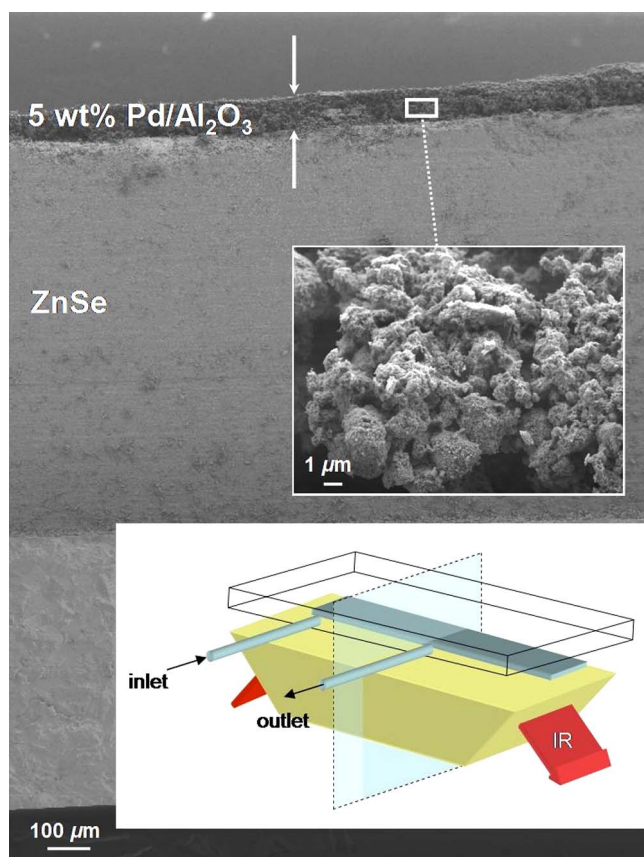


Fig. 1. Scanning electron microscopic (SEM) image of the ZnSe internal reflection element coated with a layer of 5 wt% Pd/Al₂O₃. The inset shows the porous structure of the catalyst. The thickness of the whole crystal is 2 mm. A drawing of the ATR reactor cell is also shown with the cross section along which the SEM image was taken.

required to achieve easily detectable conversion and selectivity by GC analysis. Furthermore, oxidation of alcohols on Pt-group metal catalysts has to be carried out in the mass transfer limited region in order to avoid catalyst deactivation, as discussed previously. Note also that in an early work the metal particles were intentionally located inside the narrow pores of the support to avoid catalyst deactivation [39,40]. In consideration of this point, our catalyst film is a suitable model for alcohol oxidation. Nevertheless, the effect of diffusion limitation is carefully considered throughout the present paper.

The coated IRE was installed in a home-built stainless-steel flow-through cell [41] mounted on the ATR mirror unit (Optispec) of a FTIR spectrometer (IFS-66/S, Bruker Optics). Cyclohexane solvent and alcohol solutions (18.5 mM) saturated with different gases were admitted to the catalyst at a rate of 1.0 ml min⁻¹. All experiments were carried out at 323 K. Samples were collected periodically and analyzed by GC.

The following protocol was used throughout the experiments. After background acquisition at 323 K, cyclohexane saturated with Ar was admitted into the cell for 30 min. We then reduced the catalyst in situ by admitting H₂-saturated

cyclohexane from a second glass reservoir for 30 min. We started the reaction by switching to a cyclohexane solution of an alcohol or a carbonyl compound saturated with Ar. The time required to introduce an alcohol/Pd_s (surface Pd atom) molar ratio of 1:1 over the catalytic film is ca. 5 s. After a certain reaction time (48–55 min) Ar was replaced by air in the same glass reservoir. Finally, the catalyst layer was rinsed with Ar-saturated cyclohexane to follow the desorption of weakly adsorbed species. CO adsorption was performed by the admission of CO-saturated cyclohexane (0.5 vol% CO in Ar) to the ATR cell. Moreover, control experiments with the reaction mixture on the uncoated IRE confirmed that the changes in the measured spectra were due to the presence of the catalyst layer. We recorded ATR spectra by averaging 500 scans at 4 cm⁻¹ resolution; these are presented in absorbance units as difference spectra, where the last spectrum obtained during in situ reduction of the catalyst is subtracted. Where required, spectra were corrected to compensate for the absorption of water vapor.

Transmission infrared spectra of neat and cyclohexane solutions of alcohols and carbonyl compounds (10 mM) were recorded at room temperature with a cell equipped with CaF₂ windows (Specac) by co-adding of 100 scans at a resolution of 4 cm⁻¹. Table 1 shows the assignment for the relevant vibrational modes in the 1800–1300 cm⁻¹ spectral range for neat compounds and for adsorbed carboxylate species.

2.3. Dehydrogenation in a batch reactor

The reactions were performed in a flat-bottomed, 100-ml glass reactor. Typically, 100 mg 5 wt% Pd/Al₂O₃, 1.0 g alcohol, and 30 ml cyclohexane were loaded into the reactor. Air was replaced by Ar, the reactor was immersed in a preheated oil bath, and stirring was started. For detailed conditions see Table 2. Products were analyzed by GC after 3 h.

2.4. Gas chromatographic analysis

GC analysis was carried out on a Thermo Quest Trace 2000 chromatograph, equipped with an HP-FFAP capillary column and an FID detector. Several alcohols contained the product carbonyl compound as impurities, which were taken into account during calculation of yields and selectivities. The estimated error of determination of the yields was around ±0.5–10%, depending on the yields (15–0.1%).

3. Results

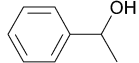
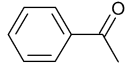
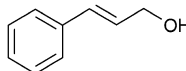
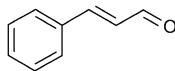
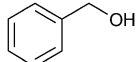
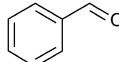
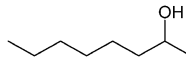
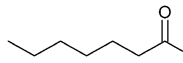
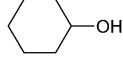
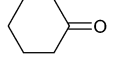
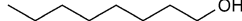
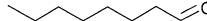
The structural effects in alcohol oxidation have been investigated in some commonly used test reactions representing various classes of alcohols. Note that an ATR-IR study of benzyl alcohol [10] and a preliminary report of cinnamyl alcohol [37] have already been published. Here we repeated

Table 1
Vibrational mode assignment for neat reactants and products, and for carboxylate species adsorbed on Al₂O₃, at 323 K

	Band assignment							
	$\nu(\text{C}=\text{O})$	$\nu(\text{C}=\text{C})$	Ring modes		$\nu_{\text{AS}}(\text{OCO})$	$\delta(\text{CH}) + \nu(\text{CC})$	$\nu_{\text{S}}(\text{OCO})$	$\delta(\text{OH})$
2-Octanol						1468 <i>m</i>		1376 <i>m</i>
2-Octanone	1727 <i>s</i>					1465 <i>m</i>		
1-Octanol						1468 <i>m</i>		1379 <i>w</i>
1-Octanal	1734 <i>s</i>					1465 <i>m</i>		
Octanoate					1552		1404	
1-Phenylethanol			1601 <i>vw</i>			1494 <i>m</i>		1368 <i>m</i>
Acetophenone	1696 <i>vs</i>		1599 <i>m</i>	1583 <i>w</i>				
Benzyl alcohol			1607 <i>vw</i>	1574 <i>vw</i>		1497 <i>m</i>		1374 <i>m</i>
Benzaldehyde	1713 <i>vs</i>		1597 <i>m</i>	1584 <i>m</i>				1390 <i>w</i>
Benzoate			1600		1547		1425 1391	
Cinnamyl alcohol			1601 <i>vw</i>	1580 <i>vw</i>		1495 <i>w</i>		1380 <i>w</i>
Cinnamaldehyde	1692 <i>vs</i>	1628 <i>m</i>	1611 <i>w</i>	1578 <i>w</i>				
Cinnamate		1643			1550		1417 1391	

vs, very strong; *s*, strong; *m*, medium; *w*, weak; *vw*, very weak.

Table 2
Dehydrogenation of aromatic and aliphatic alcohols in a batch reactor under argon. For identification of the products see Scheme 1^a

	Reactant	<i>t</i> (h)	Product	Conversion (%)	Selectivity (%)
1		3		52	92 ^b
2		3 1.5 ^d		21 13 ^d	27 ^c 57 ^d
3		5 1 ^f		23 8 ^f	54 ^e 63 ^{e,f}
4		5		0.6	100
5		3		0.5	100
6		5		0	–

^a Conditions: 0.10 g 5 wt% Pd/Al₂O₃ (without pre-reduction), 1.0 g alcohol, 30 ml cyclohexane, reflux (353 K).

^b The other product was ethyl benzene.

^c The other products were (selectivities in brackets): 3-phenyl-1-propanol (32.5%), dihydrocinnamaldehyde (1.4%), styrene (21.9%), ethyl benzene (1.3%), 1-propenylbenzene (15.7%) (see Scheme 1, where R₁=Ph-CH=C- and R₂=H).

^d Solvent: toluene, 338 K. The other products were (selectivities in brackets): 3-phenyl-1-propanol (35.4%), dihydrocinnamaldehyde (0.9%), styrene (2.1%), ethyl benzene (0.4%), 1-propenylbenzene (4.1%).

^e The other product was toluene.

^f 323 K.

the analysis under the present (improved) conditions to obtain comparable results with these key reactants.

3.1. CO adsorption

Fig. 2 shows the time-dependent ATR-IR spectra of CO adsorbed on the commercial Pd/Al₂O₃ catalyst from cyclohexane solvent. The spectra closely resemble those reported for CO on numerous supported Pd catalysts [42–44]. Two main signals were observed at 2068 and 1968 cm⁻¹, which are attributed to linear and bridged CO, respectively. A shoulder on the low-energy side of the latter signal at ca. 1900 cm⁻¹ and the evident tailing of the signal toward low

frequencies are consistent with the polycrystalline nature of the catalyst. Several adsorption sites are exposed to the solution and are probed by CO adsorption.

3.2. 2-Octanol

The in situ ATR-IR spectra presented in Fig. 3a were recorded after admission of an Ar-saturated solution of 2-octanol over the catalyst layer. The signals observed at 1377 cm⁻¹ ($\delta(\text{OH})$) and at 1468 and 1305 cm⁻¹ (alkyl chain) [45] are due to 2-octanol in solution and partly adsorbed on Al₂O₃. The negative signal at 1450 cm⁻¹ originates from uncompensated cyclohexane solvent. Formation

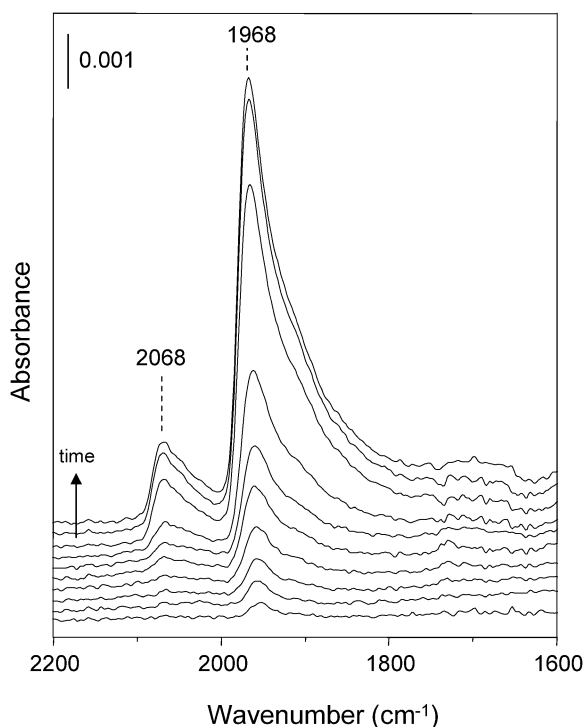


Fig. 2. In situ ATR-IR spectra of CO adsorption from CO-saturated cyclohexane (0.5 vol% CO in Ar) over Pd/Al₂O₃. The overall adsorption time was 45 min.

of 2-octanone is indicated by the appearance of the weak band at 1727 cm⁻¹ ($\nu(\text{C}=\text{O})$ of dissolved ketone; see Table 1). Similarly to the ATR spectra, GC analysis of the effluent revealed the formation of 2-octanone as the only product (0.1% yield; inset in Fig. 3).

After 55 min on stream, replacement of Ar by air resulted in a rate enhancement. The intensity of $\nu(\text{C}=\text{O})$ of 2-octanone (Fig. 3b and inset) increased sharply and reached a maximum after 61 min on stream, in good agreement with the GC analysis that showed a maximum yield of 4.9% at 62 min. In the next 20 min the yield dropped to 1.0%. It has been shown previously [37,46,47] that the rate of alcohol oxidation (dehydrogenation) on Pt-group metals can be described by a bell-shaped curve as a function of the oxidation state of the metal. When the metal (in this case, Pd) is in a reduced state and its surface is covered by hydrogen, the rate of alcohol dehydrogenation is low. This is the case at the end of the dehydrogenation of 2-octanol (Fig. 3a, bold spectrum). With the switch from Ar to air, the surface oxygen concentration increases, the adsorbed hydrogen is oxidized to water, and the rate of 2-octanol dehydrogenation increases rapidly (Fig. 3, inset). As soon as the rate of oxygen supply to the catalyst surface surpasses that of alcohol dehydrogenation, the excess oxygen covers an increasing fraction of Pd. Since the adsorption of oxygen is stronger than that of alcohols, the number of surface sites available for the adsorption and transformation of 2-octanol decreases. This process is reflected by the rapidly decreasing 2-octanone yield (Fig. 3, inset). The low reactivity of the oxidized metal surface and

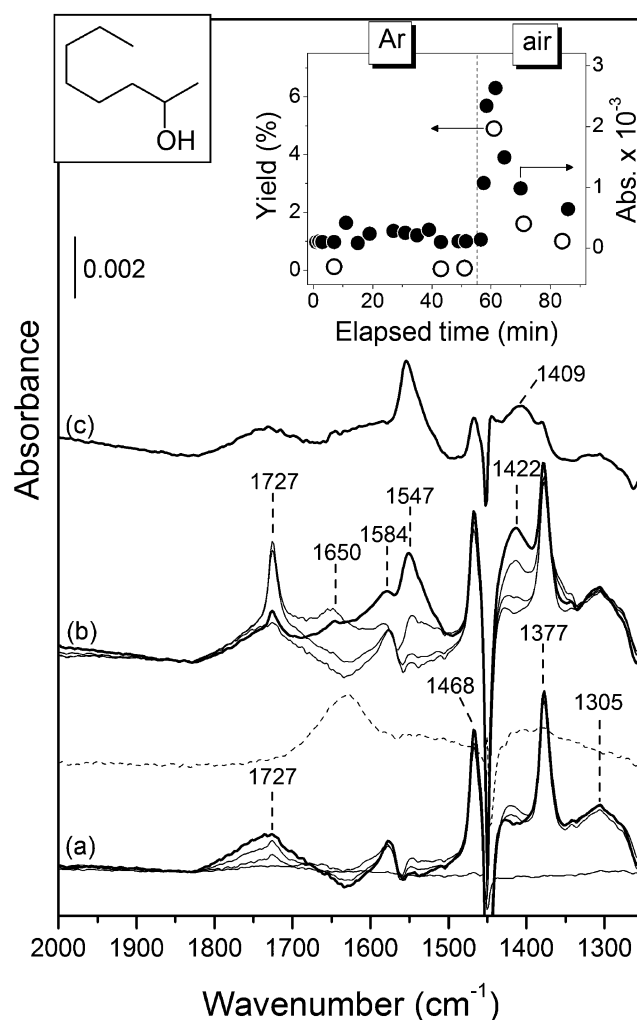


Fig. 3. In situ ATR-IR spectra recorded during dehydrogenation of 2-octanol in (a) Ar- and (b) air-saturated cyclohexane over Pd/Al₂O₃. The spectra have been collected at 0, 3, 19 and 51.5 (bold) min on stream for (a), and at 56, 58, 61, and 86 (bold) min on stream for (b). After 88 min neat solvent was passed over the catalyst layer. Spectra (c) were recorded after the catalyst layer was rinsed with Ar-saturated solvent for 30 min. The spectrum drawn with dashed line represents water accumulated by cycling H₂- and O₂-saturated solvent over the catalyst in a separate experiment. The inset shows the octanone yield (○) determined by GC and the maximum of the carbonyl signal at 1727 cm⁻¹ (●) as a function of time.

the resulting “overoxidation” of the catalyst were described many years ago [26,27].

Beside the carbonyl band, some new signals appeared in air at 1650, 1547, and 1422 cm⁻¹, and their intensity increased continuously with time (Fig. 3b). The broad signal growing at 1650 cm⁻¹ is attributed to adsorbed water that formed from the oxidation of hydrogen. The weakly polar solution of 2-octanol in cyclohexane cannot remove water that accumulates on the surface of the hydrophilic catalyst. The signals at 1547 and 1422 cm⁻¹ are assigned to the O–C–O asymmetric and symmetric stretching modes (Table 1) [48], respectively, of carboxylate species adsorbed on Al₂O₃. Since 2-octanone is highly stable against further oxidation accompanied by C–C bond breaking under the

mild conditions applied [29], the appearance of carboxylate species is probably due to impurities in 2-octanol. According to GC analysis, 2-octanol contained trace amounts of 1-octanal (< 0.1%), but its poor separation from 2-octanone, another impurity of 2-octanol, did not allow quantification. As will be shown later, 1-octanal affords octanoic acid on Pd/Al₂O₃, even in the absence of oxygen, in agreement with the development of the carboxylate bands in Fig. 3. In addition, Fig. 3a possibly reveals traces of adsorbed CO. The weak broad signal extending from 1800 to 1700 cm⁻¹ developed after admission of the Ar-saturated 2-octanol solution to the in situ reduced Pd/Al₂O₃. We assign the formation of CO to decarbonylation of 1-octanal (vide infra).

3.3. Cyclohexanol

The results for the dehydrogenation of cyclohexanol strongly resembled those discussed previously for 2-octanol. A switch from Ar-saturated to air-saturated alcohol solution resulted in a rate acceleration followed by rapid deactivation, as confirmed by ATR-IR and GC analysis. The maximum yield in Ar was 0.1%, and after Ar was replaced with air, the yield increased to 1.1% and then decreased to 0.2% within 6 min. Cyclohexanone was the only product that could be identified by GC. In the ATR-IR spectra a clear signal at 1724 cm⁻¹ and a weak signal 1698 cm⁻¹ were assigned to dissolved and adsorbed cyclohexanone, respectively. The gradually growing band of water coproduct was detected at 1625 cm⁻¹. No CO formation was observed in this case.

3.4. 1-Phenylethanol

The ATR spectra obtained after introduction of an Ar-saturated solution of 1-phenylethanol to the reactor cell are depicted in Fig. 4a. The relatively strong signals at 1494 and 1371 cm⁻¹ are attributed to 1-phenylethanol, partly dissolved and partly adsorbed on Al₂O₃. The sharp signal at 1696 cm⁻¹ reveals the formation of the dehydrogenation product acetophenone. No adsorbed CO is seen in the region above 1700 cm⁻¹; the signals above 1800 cm⁻¹ belong to dissolved 1-phenylethanol (overtone and combination bands). According to GC analysis, less than 1% acetophenone yield at about 80% selectivity was achieved in the absence of oxygen (Fig. 5). Ethyl benzene produced via C–O bond hydrogenolysis was the by-product (Scheme 1, reaction 3). The reaction rate was almost constant during the whole period.

A remarkable rate acceleration occurred when the atmosphere was changed from Ar to air, as indicated by the yield measured with GC (Fig. 5) and the intensity of the signal at 1696 cm⁻¹ (Fig. 4). At this higher acetophenone concentration, adsorption of acetophenone on Al₂O₃ is easily detectable at 1672 cm⁻¹. The frequency shift with respect to liquid acetophenone ($\Delta\nu = 24$ cm⁻¹, Table 1) is slightly higher than that observed on SiO₂ [49] and TiO₂ [50] but consistent with the value reported for SiO₂–Al₂O₃ [51] and

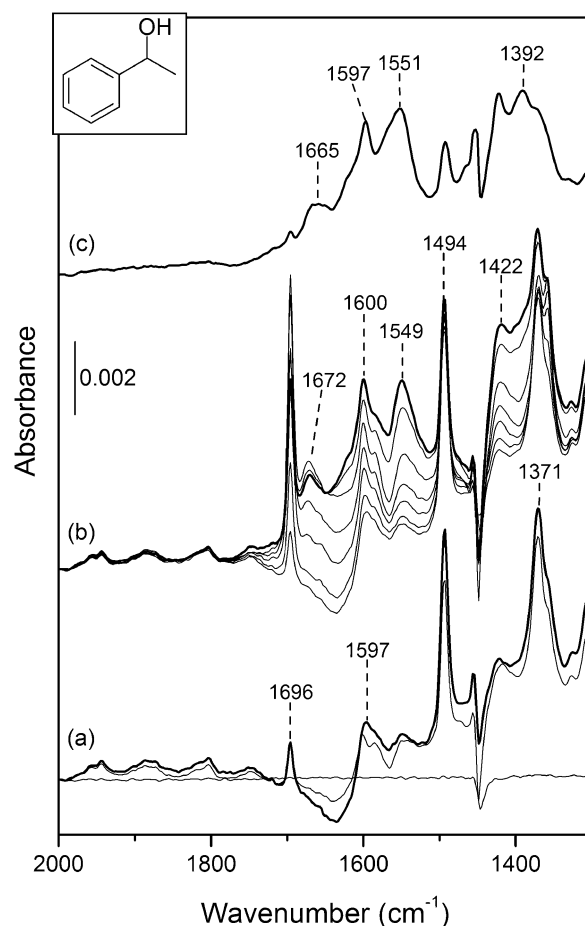


Fig. 4. In situ ATR-IR spectra recorded during dehydrogenation of 1-phenylethanol over Pd/Al₂O₃ in (a) Ar- and (b) air-saturated cyclohexane. Spectra (a) were collected at 0, 10.5 and 46.5 (bold) min on stream. Spectra (b) were collected at 48, 50, 51, 52.5, 55.5, 64.5 and 75.5 (bold) min on stream. Spectrum (c) was recorded after the catalyst layer was rinsed with Ar-saturated solvent for 35.5 min.

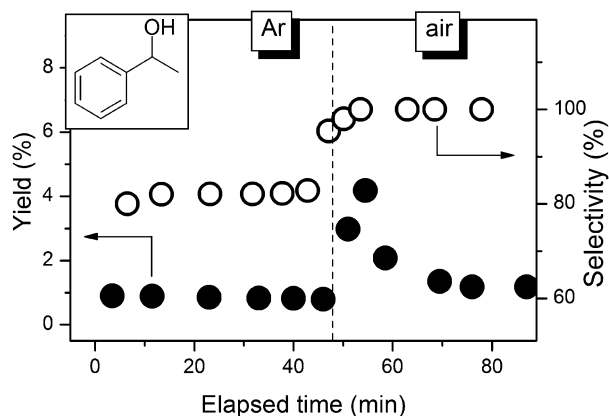


Fig. 5. Acetophenone yield (●) and selectivity (○) measured during the reaction shown in Fig. 4. The other product was ethyl benzene.

mordenite [52]. We favor the assignment to η^1 adsorption on Al₂O₃, though adsorption on Pd is also feasible, since similar values were reported for adsorption on metals with Pd/SiO₂ [53] and Pt/SiO₂ [54].

After 55 min on stream, the rate of oxidative dehydrogenation decreased, the intensity of the signals at 1696 and 1672 cm^{-1} was attenuated, and the yield decreased to 2.1%. The explanation is again the increasing oxygen concentration at the Pd surface, leading to “overoxidation.” The high oxygen concentration is indicated by the 100% selectivity in this region (Fig. 5) due to complete oxidation of hydrogen and the cease of C–O bond hydrogenolysis.

Accumulation of water is indicated by the growing baseline between 1700 and 1500 cm^{-1} . Furthermore, carboxylate species adsorbed on Al_2O_3 are shown by signals at 1549 and 1422 cm^{-1} . Though very weak, these signals are already visible under Ar and strongly enhanced in the presence of oxygen. The signal at 1549 cm^{-1} displays a noticeable, short time delay with respect to the growing baseline with its center at ca. 1622 cm^{-1} (water). After the baseline is almost stabilized, the signal at 1549 cm^{-1} grows faster, indicating that water formation and carboxylate formation are consecutive processes. Similarly to the oxidation of 2-octanol, the presence of carboxylate species is attributed to the presence of impurities in the reactant. The commercially available 1-phenylethanol contained traces of phenyl acetaldehyde (beside acetophenone and ethyl benzene). Since the boiling points of the carbonyl compounds are very similar, further purification was not considered. Note also the high sensitivity of the ATR-IR method; the carboxylic acid by-product could not be detected by GC analysis.

No CO was detected during dehydrogenation and oxidation of 1-phenylethanol. In a control experiment, acetophenone instead of 1-phenylethanol saturated with hydrogen and then with air was passed over the catalyst layer. No CO could be detected independently of the presence or absence of oxygen, confirming that decarbonylation of ketones is not feasible under the mild conditions applied here.

3.5. 1-Octanol

When the Ar-saturated solution of 1-octanol was brought into contact with $\text{Pd}/\text{Al}_2\text{O}_3$, a weak broad band developed immediately at 1808 cm^{-1} , which shifted with time to 1820 cm^{-1} (Fig. 6a). This band partly overlaps with a similarly developing broad band at 1738 cm^{-1} . The shape and position of the bands suggest that they can be assigned to CO multi-bonded to polycrystalline metallic Pd [55]. In addition, signals of 1-octanol (dissolved and partly adsorbed on Al_2O_3) are found at 1468 and 1380 cm^{-1} . Very weak bands of O–C–O groups are also found at 1546, 1422, and 1303 cm^{-1} . Interestingly, no characteristic signal of 1-octanol could be detected at around 1730 cm^{-1} . The absence of 1-octanol in the liquid phase was confirmed by GC analysis. The probable explanation for the absence of 1-octanol and the presence of small amounts of CO and octanoic acid is that 1-octanol dehydrogenation occurred at a very low rate, and the aldehyde was consumed rapidly by decarbony-

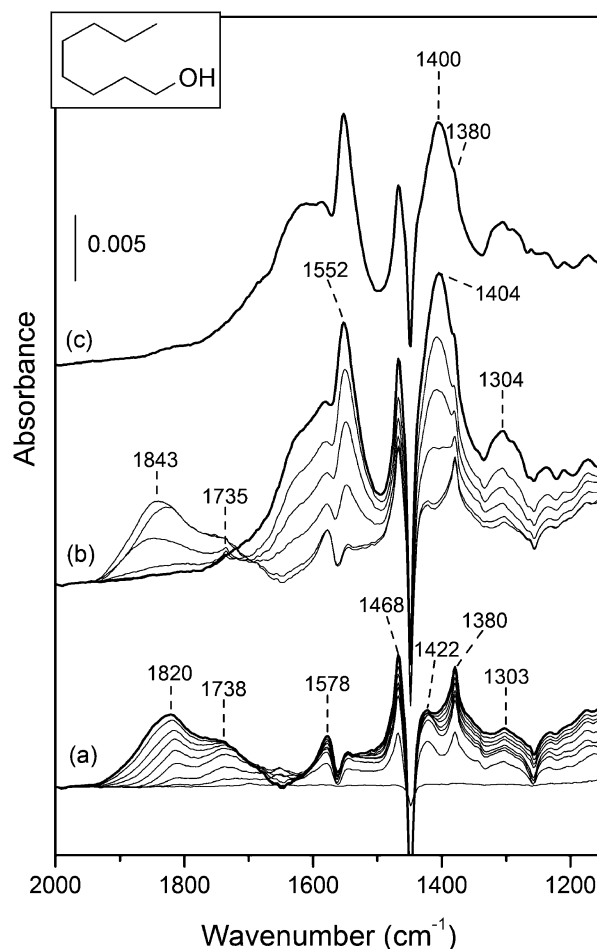


Fig. 6. In situ ATR-IR spectra recorded during dehydrogenation of 1-octanol over $\text{Pd}/\text{Al}_2\text{O}_3$ in (a) Ar- and (b) air-saturated solvent. Spectra (a) have been collected at 0, 1, 2, 4.5, 9, 16, 23.5, 33.5 and 40 (bold) min on stream. Spectra (b) have been collected at 46, 47, 49.5, 51, 55 and 77 (bold) min on stream. Spectrum (c) was recorded after the catalyst layer was rinsed with Ar-saturated solvent for 23.5 min.

lation and further oxidation on Pd and by disproportionation on the basic sites of Al_2O_3 [10,56] (see Scheme 1, reaction 5).

After replacement of Ar by air (Fig. 6b), a weak signal of 1-octanol appeared at 1735 cm^{-1} , the band of adsorbed CO disappeared, and the amount of octanoate on Al_2O_3 increased. GC analysis at 8.5 min after the switch to air showed only 1-octanol in the effluent at 1.3% yield. Subsequently, the amount of 1-octanol diminished, as indicated by the attenuated intensity of the signal at 1735 cm^{-1} and the lower yield in the effluent (0.75% after 27 min on stream under air). Similarly to the oxidative dehydrogenation of 2-octanol and 1-phenylethanol, a broad band due to water accumulation on the catalyst surface developed continuously between ca. 1700 cm^{-1} and 1500 cm^{-1} that did not desorb during rinsing with neat solvent (Fig. 6c). This observation is not surprising if we consider the strikingly different empirical solvent parameters of the solvent cyclohexane ($E_T^N = 0.006$) and water ($E_T^N = 1.0$) [57].

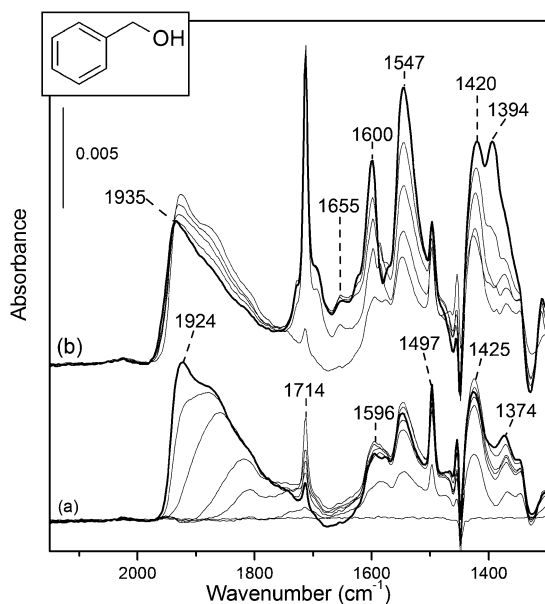


Fig. 7. In situ ATR-IR spectra recorded during dehydrogenation of benzyl alcohol over Pd/Al₂O₃ in (a) Ar- and (b) air-saturated solvent. Spectra (a) have been collected at 0, 1, 2, 3, 7, 16.5 and 40 (bold) min on stream. Spectra (b) have been collected at 51, 57.5, 63.5, 74.5 and 96.5 (bold) min on stream.

3.6. Benzyl alcohol

The spectra obtained during dehydrogenation and oxidation of the simplest aromatic primary alcohol, benzyl alcohol, are collected in Fig. 7. Assignment of the bands has been published elsewhere [10]. Briefly, under an inert atmosphere (Fig. 7a) benzyl alcohol dehydrogenated readily, affording benzaldehyde, as confirmed by the IR signal at 1714 cm⁻¹ (ν (C=O)) and GC analysis. The considerable amount of CO is indicated by the bands centered at 1924 and 1879 cm⁻¹. After the introduction of air (Fig. 7b), the signal at 1714 cm⁻¹ increased and then decreased only slightly after about 30 min. A similar behavior was found by GC analysis. A comparison of the GC and ATR-IR data reveals an interesting situation: despite the high oxygen concentration in the feed, the surface CO coverage is considerable and the catalyst deactivation is moderate.

Furthermore, benzoate species characterized by bands at 1600, 1547, and 1425 cm⁻¹ developed already under Ar, and their intensity increased under air. Benzoic acid could not be detected by GC, and the fate of the hydrocarbon fragment, a coproduct of the decarbonylation reaction, remained unknown (Scheme 1, reaction 2). The presence of small amounts of toluene in the effluent confirmed hydrogenolysis of benzyl alcohol on the reduced Pd surface. This side reaction dropped to a low level in the presence of air.

3.7. Decarbonylation of 1-octanal and benzaldehyde

To better understand the structural effects on the decarbonylation of aldehydes, we investigated the interac-

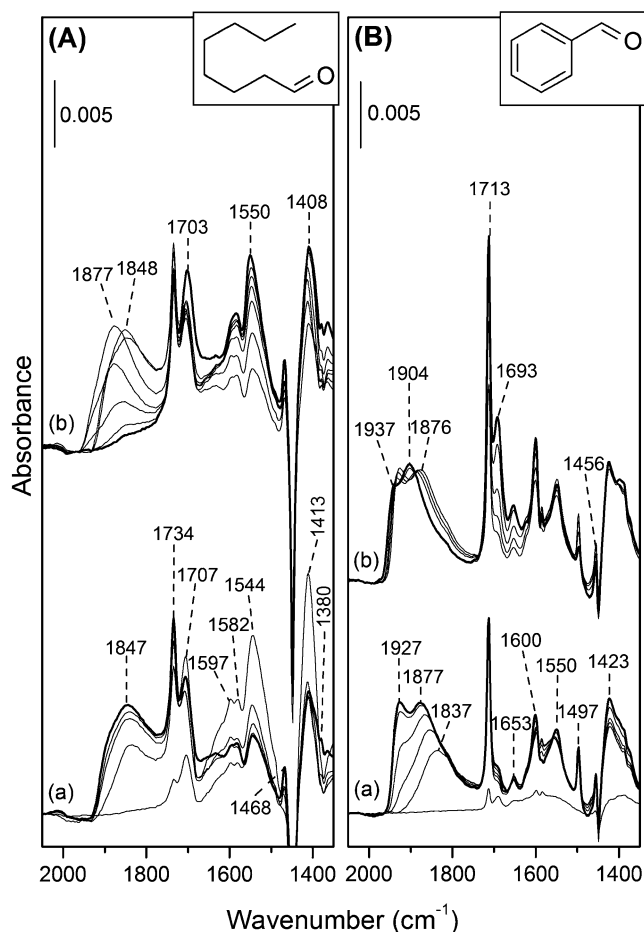


Fig. 8. Comparison of CO formation during decarbonylation of 1-octanal (Panel A) and benzaldehyde (Panel B) over Pd/Al₂O₃. Spectra have been collected when H₂-(a) then air-(b) saturated aldehyde solutions were passed over the catalyst layer. (A) Spectra (a) were recorded at 0, 1, 2, 7.5 and 27.5 (bold) min on stream. Spectra (b) were recorded at 31, 36, 37, 38, 39, 42 and 57 (bold) min on stream. (B) Spectra (a) were recorded at 0, 6, 9.5, 14, 23.5 and 36.5 (bold) min on stream. Spectra (b) were recorded at 40, 43.5, 45.5, 52 and 62.5 (bold) min on stream.

tion of prerduced Pd/Al₂O₃ with H₂-saturated solutions of 1-octanal and benzaldehyde. Since there was no alcohol present as a reducing agent in the feed, Ar was replaced by hydrogen to maintain reducing conditions. The ATR spectra in Figs. 8A and B show bands at 1734 and 1707, and 1713 and 1693 cm⁻¹, which are attributed to dissolved and adsorbed 1-octanal and benzaldehyde, respectively [58]. CO bands developed at 1847 cm⁻¹ with a clear shoulder close to 1900 cm⁻¹ for 1-octanal and at 1927, 1877, and 1837 cm⁻¹ for benzaldehyde. Compared with the case of an Ar-saturated solution of benzaldehyde [10], Fig. 9b reveals a different reactivity of benzaldehyde under continuously reducing conditions, which is reflected in a higher CO coverage and a different band shape.

The presence of octanoate and benzoate species adsorbed on Al₂O₃ is also clear from the set of signals appearing below 1650 cm⁻¹, as discussed for 1-octanol and benzyl alcohol (see also Table 1). Signals at 1468 cm⁻¹ (Fig. 8A)

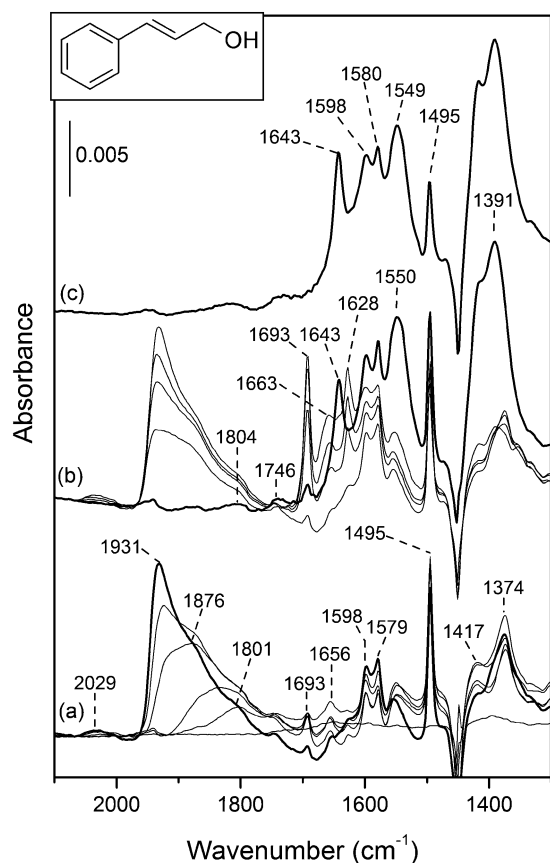


Fig. 9. In situ ATR-IR spectra recorded during dehydrogenation of cinnamyl alcohol over Pd/Al₂O₃ in (a) Ar- and (b) air-saturated solvent. Spectra (a) have been collected at 0, 2, 4.5, 10.5, 16.5 and 45 (bold) min on stream. Spectra (b) have been collected at 51, 53, 54.5, 58.5 and 93.5 (bold) min on stream.

and at 1497 cm⁻¹ (Fig. 8B) are diagnostic for 1-octanol and benzyl alcohol, respectively. Formation of the corresponding alcohol is mainly due to C=O bond hydrogenation, but also partly to disproportionation of the aldehyde catalyzed by Al₂O₃ (Cannizzaro reaction) [10,56]. GC analysis indicated the presence of trace amounts of octanoic acid in the effluent, but benzoic acid could not be detected.

Evolution of the strong CO signals above 1800 cm⁻¹ confirms decarbonylation of both aldehydes on reduced Pd. The different behaviors of benzaldehyde and 1-octanal in the presence of air (spectra b) is in agreement with the results obtained during oxidation of the corresponding alcohols (Figs. 6 and 7). Carbon monoxide formed from 1-octanal is rapidly and almost completely removed by air (Fig. 8A). In the case of benzaldehyde the CO bands are shifted toward higher frequency by a switch from hydrogen to air, but the intensity of the bands is barely influenced, and an almost constant, high CO coverage remained on the Pd surface. Obviously, decarbonylation of benzaldehyde on the free metallic sites and oxidative removal of CO occur in parallel. Since the concentrations of the two aldehydes in solution are identical and the decarbonylation rates are comparable, it seems that CO adsorbed on Pd in the presence of

1-octanol, and its dehydrogenated products are more easily oxidized. We can also conclude that the small amount of CO that evolved during dehydrogenation of 1-octanol (Fig. 6) is due to the low rate of dehydrogenation to 1-octanol and not to the slow decarbonylation of 1-octanal.

3.8. Cinnamyl alcohol

Oxidation of cinnamyl alcohol is a commonly used test reaction for the dehydrogenation of allylic alcohols. When the Ar-saturated solution of cinnamyl alcohol (Fig. 9a) was admitted to the reactor cell, strong bands developed at 1801, 1876, and 1931 cm⁻¹, which are assigned to multicoordinated CO, as already observed in a previous study [37]. A small fraction of linearly bonded CO can also be seen at 2029 cm⁻¹. The signals appearing below 1700 cm⁻¹ are assigned to cinnamaldehyde (1693 cm⁻¹), cinnamyl alcohol (1598, 1579, 1495, and 1374 cm⁻¹), and carboxylate species on Al₂O₃ (1552 and 1417 cm⁻¹). These signals confirm dehydrogenation of cinnamyl alcohol to cinnamaldehyde, followed by the fast decarbonylation of the latter.

GC analysis after 8 min on stream indicated 4.2% conversion and the formation of two major products: cinnamaldehyde with 47% selectivity and 3-phenyl-1-propanol with 39% selectivity. In addition, dihydrocinnamaldehyde (2.2%), 1-propenylbenzene (7.8%), ethyl benzene (0.8%), and styrene (3.0%) were also detected. After a short initial period, the activity of the catalyst decreased monotonously in Ar. Despite the high selectivity for 3-phenyl-1-propanol, no signal in Fig. 9a can be unequivocally assigned to this alcohol, because of its close resemblance to cinnamyl alcohol.

After Ar was replaced with air, the aldehyde signal at 1693 cm⁻¹ ($\nu(\text{C}=\text{O})$) and 1628 cm⁻¹ ($\nu(\text{C}=\text{C})$) increased (Fig. 9b), in agreement with the 12-fold enhancement in catalytic activity, determined by GC. A signal is also found at ca. 1663 cm⁻¹, which is assigned to the hydrogen-bonded carbonyl group of adsorbed cinnamaldehyde. The CO signals decreased gradually and completely disappeared with time, whereas the intensity of the $\nu(\text{C}=\text{O})$ started to drop only after ca. 15 min on stream. After replacement of Ar by air, the amount of ethyl benzene and styrene increased in the effluent, as a result of the higher rate of cinnamaldehyde formation and decarbonylation. This observation is very important, since this is the only case where the hydrocarbons formed by decarbonylation of an aldehyde [via the strongly adsorbed R_{ad} species; Eqs. (2) and (4)] could be detected unambiguously.

Careful analysis of the 1700–1500 cm⁻¹ spectral region in the presence of air (Fig. 9b) reveals the formation of carboxylate species. The signals belonging to adsorbed cinnamate appear with a delay of about 10 min with respect to the increasing baseline assigned to water (ca. 1630 cm⁻¹). This is clear from the sharp band at 1643 cm⁻¹ ($\nu(\text{C}=\text{C})$, aliphatic chain, Table 1) and the rapid increase in intensity of the bands at 1550 and 1391 cm⁻¹. Probably as a result of the appearance of these bands, the broad band of water at

ca. 1630 cm^{-1} is attenuated and is followed by a decrease in the signals at 1693 and 1663 cm^{-1} , indicating smaller amounts of adsorbed cinnamaldehyde. These changes may be interpreted as the formation of cinnamic acid via aldehyde hydration and subsequent dehydrogenation over the Pd surface.

3.9. ATR-IR reactor vs. batch reactor

Dehydrogenation of all six alcohols was repeated in a batch reactor under conditions similar to those applied in the ATR-IR cell serving as continuous-flow reactor. The results collected in Table 2 confirm that the reactivity of aromatic alcohols is up to two orders of magnitude higher than that of the aliphatic alcohols, in agreement with earlier observations [59,60]. The average rate of the dehydrogenation of the secondary aromatic alcohol (1-phenylethanol) was higher than that of the primary aromatic (benzyl alcohol) and allylic (cinnamyl alcohol) alcohols. The product distributions were similar to those obtained in the ATR-IR cell (Scheme 1). Interestingly, in the continuous-flow reactor the primary aromatic alcohols reacted faster initially under Ar, but their reactivity dropped after about 10 min. Dehydrogenation of 1-phenylethanol proceeded more slowly, but deactivation was barely detectable (Fig. 5). This difference in the reactivities of aromatic alcohols is attributed to the different conversions and to the remarkably different mass transports in the two reactor types.

4. Discussion

4.1. Decarbonylation of aldehydes

Gas chromatographic analysis of the effluent of the continuous-flow reactor identified by-products originating from hydrogenation and hydrogenolysis-type side reactions (Scheme 1) in the dehydrogenation of 1-phenylethanol, benzyl alcohol, and cinnamyl alcohol, even in the presence of molecular oxygen. An example is shown in Fig. 5: formation of acetophenone from 1-phenylethanol was always accompanied by hydrogenolysis of the reactant to ethyl benzene. These observations strongly support the mostly accepted dehydrogenation mechanism of the aerobic oxidation of alcohols, that is, the reactions proceed on metallic surface sites, and the major role of oxygen is the oxidation of the coproduct hydrogen (and possibly some other surface impurities), thus accelerating alcohol dehydrogenation [14–18]. The presence of Pd^0 surface sites is supported also by an important side reaction, the facile decarbonylation of aldehydes.

The relevant difference between the alcohols lies in the stability of the product carbonyl compounds. Aldehydes decarbonylate easily on metallic Pd sites to form CO, hydrogen, and a hydrocarbon fragment [11,12]. Under the conditions applied here, none of the ketones formed from

the secondary alcohols (2-octanol, 1-phenylethanol, cyclohexanol) decarbonylated on $\text{Pd}/\text{Al}_2\text{O}_3$. These results are in agreement with those of former IR studies in aqueous acidic medium [34] but contradict UHV studies on single crystal Pd surfaces [33]. In the latter case even the simplest secondary aliphatic alcohol, 2-propanol, decarbonylated on Pd(111). Previous ATR-IR studies in apolar organic solvents had documented the decarbonylation of cinnamyl and benzyl alcohols [10,37]. The present work clearly shows that CO is generally formed when the oxidation product is an aldehyde. The ATR spectra do not give evidence for the presence of the hydrocarbon fragments originating from decarbonylation, either because their signals may overlap with others in the already crowded $1700\text{--}1300\text{ cm}^{-1}$ region or because they are removed from the surface, as indicated by the formation of ethyl benzene and styrene during cinnamyl alcohol oxidation.

Both CO and the hydrocarbon residue adsorb strongly on Pd and can cause deactivation by site blocking. Removal of the hydrocarbon residue from the surface requires hydrogen, that is, reducing conditions. In contrast, the complete and fast removal of CO necessitates adsorbed oxygen. A remarkable feature of the aerobic oxidation of alcohols on Pd (and other Pt-group metals) is that under appropriate conditions the two processes may run parallel, allowing a reasonably high rate of alcohol oxidation. A representative example of this situation is the oxidation of benzyl alcohol (Fig. 7). Despite the continuous and rapid decarbonylation of benzaldehyde, dehydrogenation of the alcohol is barely hindered by this side reaction. Obviously, the explanation for this is the dehydrogenation mechanism of alcohol oxidation; that is, there is adsorbed oxygen and hydrogen present on the reduced metal surface. In this respect, the simultaneous reductive and oxidative removal of hydrocarbon fragments and CO, respectively, is similar to the competing oxidation of hydrogen by adsorbed oxygen and the hydrogenation of the reactant by the rest of adsorbed hydrogen (Scheme 1).

It is possible that the aerobic oxidation of benzyl alcohol represents an “ideal” case, and in many other reactions the simultaneous removal of the hydrocarbon fragment and CO is sluggish or requires conditions that are difficult to find in practical catalysis. This situation could provide a feasible explanation for the frequently observed strong deactivation of supported Pt-group metals during aerobic oxidation of alcohols and for the sometimes excellent reaction rates achieved in the same reactions after a careful optimization of the reaction conditions [16].

The shape and position of the CO bands developed during oxidation of benzyl alcohol (Fig. 7), 1-octanol (Fig. 6), and, to a lesser extent, cinnamyl alcohol (Fig. 9) are significantly different from those of (diluted) CO dissolved in the solvent (Fig. 2). Note, for example, the almost complete absence of the signal due to linear CO during the oxidation reactions. It has been shown that the presence of other species can affect the appearance of the signals on well-defined Pd nanoparticles [61]. When CO is formed by decomposition of the

aldehyde product, the metal surface is partially covered by hydrogen, oxygen, alcohol, aldehyde, carboxylic acid, water, hydrocarbon fragments, and solvent. Clearly, many of these species can influence the adsorption mode and strength of CO on Pd/Al₂O₃ and thus the position and shape of the IR band.

4.2. The role of water coproduct

An interesting observation is that the rate of dehydrogenation increases sharply with a switch from Ar-saturated to air-saturated alcohol solutions, but the conversion drops rapidly after the maximum, in line with a recent report [36]. The conversion of all six alcohols in the continuous-flow reactor is plotted in Fig. 10 to help comparison. The explanation for the sharp maxima within 10–15 min after the switch from Ar to air is the continuous increase in the actual oxygen concentration on the Pd surface, as discussed previously in connection with the oxidation of 2-octanol (Fig. 3). The only exception to this is the oxidation of benzyl alcohol, which is characterized by a high rate on a broader time scale. The exceptional behavior of benzyl alcohol may be connected with another phenomenon, the accumulation of water coproduct on the catalyst surface and the role of polarity (or hydrophilic/hydrophobic character) of the alcohol substrate.

Water plays a key role in the reaction network. It forms from the oxidation of hydrogen in amounts equimolar to the carbonyl compound. Water available at the catalyst sur-

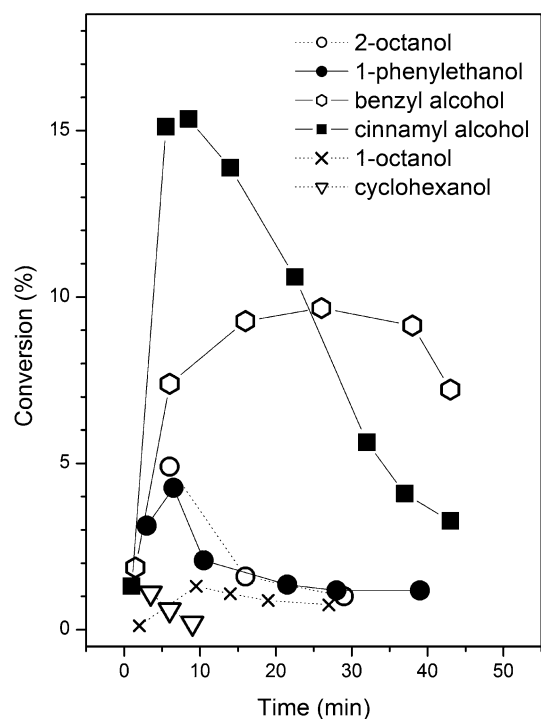


Fig. 10. Conversion of 1- and 2-octanol, cyclohexanol, 1-phenylethanol, and benzyl and cinnamyl alcohols measured during aerobic oxidation in the continuous-flow reactor. Zero time corresponds to the switch from Ar to air.

face accelerates the further oxidation of aldehydes to carboxylic acids as hydration of the carbonyl group and the subsequent dehydrogenation of the geminal diol is faster than the direct oxidation route [27,29]. Water may also form by hydrogenolysis of the C–O bond of the alcohol substrate (Scheme 1, reaction 3). In a non-aqueous medium that is a reasonable choice for water-insoluble alcohols and is generally favored for the synthesis of aldehydes, rapid removal of water from the catalyst surface may be critical. The ATR-IR spectra clearly indicated the accumulation of water on the catalyst surface. The alcohol substrate has to compete with water for the surface sites, and even its diffusion through the aqueous “layer” at the catalyst surface may reduce the overall reaction rate. Among the six alcohols investigated here, benzyl alcohol is the most polar ($E_T^N = 0.608$ [57]) and may enhance the solubility of water in the reaction medium at the low conversions achieved in the continuous-reactor cell. This effect is indicated by the relatively moderate accumulation of water on the catalyst surface during benzyl alcohol oxidation, as shown in the spectra in Fig. 7b. Note that on a laboratory scale, removal of water is simply achieved by working close to the reflux temperature. This solution has the further advantage that the risk of explosion of the organic solvent-air mixture is minimized.

5. Conclusions

A major conclusion of the present work is that decarbonylation of the product aldehyde is a general feature of the oxidation of primary aliphatic, allylic, and aromatic alcohols on Pd. The complete oxidative removal of CO and the hydrocarbon coproduct is not a necessary requirement for achieving good reaction rates in the oxidative dehydrogenation of alcohols. An important consequence of this observation is that a feasible kinetic model of the reaction should involve the partial coverage of the surface sites by CO and the hydrocarbon fragment [Eqs. (1) and (2)], in addition to the reactant alcohol, the product aldehyde, and hydrogen and oxygen.

In addition to the sensitive detection of CO, the in situ ATR-IR spectroscopic analysis allowed the unambiguous recognition of carboxylate species, even at very low alcohol conversion. At low conversion the small amount of carboxylic acid adsorbed strongly on the catalyst surface (mainly on Al₂O₃), and it was not detectable in the liquid phase by GC analysis.

Acknowledgments

The authors gratefully acknowledge the financial support of the ETH Zurich and the Foundation Claude and Giuliana. We thank Dr. F. Krumeich for the TEM and SEM measurements.

References

- [1] B.M. Weckhuysen, *In-situ Spectroscopy of Catalysts*, American Scientific Publishers, Stevenson Ranch, CA, 2004.
- [2] A. Brückner, *Catal. Rev.-Sci. Eng.* 45 (2003) 97.
- [3] N.J. Harrick, *Internal Reflection Spectroscopy*, Interscience, New York, 1967.
- [4] T. Bürgi, A. Baiker, *J. Phys. Chem. B* 106 (2002) 10649.
- [5] D. Ferri, S. Frauchiger, T. Bürgi, A. Baiker, *J. Catal.* 219 (2003) 425.
- [6] I. Ortiz-Hernandez, C.T. Williams, *Langmuir* 19 (2003) 2956.
- [7] G. Mul, G.M. Hamminga, J.A. Moulijn, *Vibr. Spectrosc.* 34 (2004) 109.
- [8] A. Gisler, T. Bürgi, A. Baiker, *J. Catal.* 222 (2004) 461.
- [9] T. Bürgi, *J. Catal.* 229 (2005) 55.
- [10] C. Keresszegi, D. Ferri, T. Mallat, A. Baiker, *J. Phys. Chem. B* 109 (2005) 958.
- [11] J.L. Davis, M.A. Barteau, *Surf. Sci.* 187 (1987) 387.
- [12] J.L. Davis, M.A. Barteau, *J. Am. Chem. Soc.* 111 (1989) 1782.
- [13] R. Shekhar, M.A. Barteau, R.V. Plank, J.M. Vohs, *J. Phys. Chem. B* 101 (1997) 7939.
- [14] P. Vinke, D. de Wit, A.T.J.W. de Goede, H. van Bekkum, *Stud. Surf. Sci. Catal.* 72 (1992) 1.
- [15] M. Besson, P. Gallezot, *Catal. Today* 57 (2000) 127.
- [16] T. Mallat, A. Baiker, *Chem. Rev.* 104 (2004) 3037.
- [17] H. Wieland, *Berichte d. D. Chem. Ges.* 46 (1913) 3327.
- [18] K. Heyns, H. Paulsen, *Adv. Carbohydr. Chem.* 17 (1962) 169.
- [19] J.M.H. Dirkx, H.S. van der Baan, M.A.J.J. van der Broek, *Carbohydr. Res.* 59 (1977) 63.
- [20] E. Müller, K. Schwabe, *Kolloid Z.* 52 (1930) 163.
- [21] T. Mallat, A. Baiker, *Catal. Today* 24 (1995) 143.
- [22] A.P. Markusse, B.F.M. Kuster, D.C. Koningsberger, G.B. Marin, *Catal. Lett.* 55 (1998) 141.
- [23] J.-D. Grunwaldt, C. Keresszegi, T. Mallat, A. Baiker, *J. Catal.* 213 (2003) 291.
- [24] J.H.J. Kluytmans, A.P. Markusse, B.F.M. Kuster, G.B. Marin, J.C. Schouten, *Catal. Today* 57 (2000) 143.
- [25] A.F. Lee, K. Wilson, *Green Chem.* 6 (2004) 37.
- [26] P. Vinke, H.E. van Dam, H. van Bekkum, *Stud. Surf. Sci. Catal.* 55 (1990) 147.
- [27] H.E. van Dam, A.P.G. Kieboom, H. van Bekkum, *Appl. Catal.* 33 (1987) 361.
- [28] R. DiCosimo, G.M. Whitesides, *J. Phys. Chem.* 93 (1989) 768.
- [29] T. Mallat, A. Baiker, *Catal. Today* 19 (1994) 247.
- [30] R.S. Goncalves, J.-M. Leger, C. Lamy, *Electrochim. Acta* 33 (1988) 1581.
- [31] R. Parsons, T. VanderNoot, *J. Electroanal. Chem.* 257 (1988) 9.
- [32] J.L. Davis, M.A. Barteau, *Surf. Sci.* 197 (1988) 123.
- [33] J.L. Davis, M.A. Barteau, *Surf. Sci.* 235 (1990) 235.
- [34] L.-W. Leung, M.J. Weaver, *Langmuir* 6 (1990) 323.
- [35] R.M. Souto, J.L. Rodriguez, E. Pastor, T. Iwasita, *Langmuir* 16 (2000) 8456.
- [36] T. Bürgi, M. Bieri, *J. Phys. Chem. B* 108 (2004) 13364.
- [37] C. Keresszegi, T. Bürgi, T. Mallat, A. Baiker, *J. Catal.* 211 (2002) 244.
- [38] A. Borodzinski, M. Bonarowska, *Langmuir* 13 (1997) 5613.
- [39] H.E. van Dam, H. van Bekkum, *React. Kinet. Catal. Lett.* 40 (1989) 13.
- [40] H.E. van Dam, P. Duijverman, A.P.G. Kieboom, H. van Bekkum, *Appl. Catal.* 33 (1987) 373.
- [41] T. Bürgi, R. Wirz, A. Baiker, *J. Phys. Chem. B* 107 (2003) 6774.
- [42] A. Palazov, C.C. Hang, R.J. Kokes, *J. Catal.* 36 (1975) 338.
- [43] P. Gelin, A.R. Siedle, J.T. Yates, *J. Phys. Chem.* 88 (1984) 2978.
- [44] N. Sheppard, C. de la Cruz, *Adv. Catal.* 41 (1996) 1.
- [45] L.J. Bellamy, *Infrared Spectra of Complex Molecules*, third ed., Wiley, New York, 1975.
- [46] T. Mallat, Z. Bodnar, P. Hug, A. Baiker, *J. Catal.* 153 (1995) 131.
- [47] T. Mallat, C. Brönnimann, A. Baiker, *Appl. Catal. A* 149 (1997) 103.
- [48] K. Nakamoto, *Infrared and Raman Spectra of Inorganic and Coordination Compounds*, Wiley, New York, 1986, p. 231.
- [49] I. Ahmad, T.J. Dines, J.A. Anderson, C.H. Rochester, *J. Colloid Interface Sci.* 195 (1997) 216.
- [50] I. Ahmad, J.A. Anderson, T.J. Dines, C.H. Rochester, *Spectrochim. Acta A* 54 (1998) 319.
- [51] I. Ahmad, J.A. Anderson, C.H. Rochester, T.J. Dines, *J. Mol. Catal. A* 135 (1998) 63.
- [52] I. Ahmad, J.A. Anderson, T.J. Dines, C.H. Rochester, *J. Colloid Interface Sci.* 207 (1998) 371.
- [53] H.W. Chen, C.S. Chen, S.J. Harn, *J. Phys. Chem.* 99 (1995) 10557.
- [54] C.S. Chen, H.W. Chen, W.H. Cheng, *Appl. Catal. A* 248 (2003) 117.
- [55] F.M. Hoffmann, *Surf. Sci. Reports* 3 (1983) 107.
- [56] A.E.T. Kuiper, J. Medema, J.J.G.M. van Bokhoven, *J. Catal.* 29 (1973) 40.
- [57] C. Reichardt, *Solvents and Solvent Effects in Organic Chemistry*, third ed., Wiley-VCH, Weinheim, 2003, p. 418.
- [58] J. Kondo, N. Ding, K. Maruya, K. Domen, T. Yokoyama, N. Fujita, T. Maki, *Bull. Chem. Soc. Jpn.* 66 (1993) 3085.
- [59] M. Hayashi, K. Yamada, S. Nakayama, *J. Chem. Soc., Perkin Trans. 1* (2000) 1501.
- [60] C. Keresszegi, T. Mallat, A. Baiker, *New J. Chem.* 25 (2001) 1163.
- [61] S. Schauerhann, J. Hoffmann, V. Johaneck, J. Hartmann, J. Libuda, H.J. Freund, *Angew. Chem. Int. Ed.* 41 (2002) 2532.